Functionalized ceramic nanofilter for wastewater treatment by coupling membrane separation and catalytic ozonation

Clémentine Mansas, Loubna Atfane-Karfane, Eddy Petit, Julie Mendret, Stéphan Brosillon, André Ayral

Functionalized ceramic nanofilter for wastewater treatment by coupling membrane separation and catalytic ozonation

Clémentine Mansas, Loubna Atfane-Karfane, Eddy Petit, Julie Mendret, Stéphan Brosillon, André Ayral

Institut Européen des Membranes, IEM – UMR 5635, ENSCM, CNRS, Univ Montpellier, Place Eugène Bataillon, Montpellier, France

Abstract

Micropollutants elimination in water becomes a global concern and represents an important issue for a possible reuse or a release to the environment. Hybrid processes combining membrane filtration and catalytic ozonation offer promising opportunities for micropollutant removal. A ceramic commercial nanofilter with a very low molecular weight cut-off of 200 Da was functionalized by sol-gel deposition of a mesoporous maghemite (γ-Fe_2O_3) thin layer. Preliminary experiments enabled to determine the maximum temperature usable for the thermal strengthening of the catalytic layer without significant permeance change. The catalytic activity of the iron oxide equivalent powder was tested in batch reactor with ozone and para-chlorobenzoic acid (pCBA) which quickly reacts with hydroxyl radicals formed with ozone at the catalyst surface, and only very slowly with ozone itself. The operational performance of the functionalized ceramic membrane was evaluated in a dedicated pilot. The obtained results unequivocally show the catalytic activity of this functionalized membrane.

Keywords: ceramic nanofilters, catalytic ozonation, hybrid process, Fe_2O_3 catalyst, micropollutant elimination

1. Introduction

Water treatment and reuse are key topics with respect to the scarcity of drinking water on earth [1], [2]. A global concern is associated with the elimination of organic micropollutants before a possible reuse or a discharge in the environment [3], [4]. Different technologies are implemented for tertiary water treatment including filtration processes (using fixed beds or membranes) and advanced oxidation processes like ozonation [5]–[11].

Combining membrane separation and catalytic ozonation is a promising technology for micropollutant removal [12]. This should especially be the case when the separative surface of a nanofiltration (NF) membrane is functionalized in order to act as catalytic contactor. Oxidation by ozone can indeed be enhanced by using a suitable catalyst. Catalytic ozonation is mainly based on heterogeneous catalysis; the active solids are usually metals or metal oxides [12]–[16]. Two types of NF membranes are available, organic and inorganic membranes. With organic membranes it is difficult to deposit a continuous and stable catalytic layer because of different factors, especially the very limited thermal stability and the very high mechanical flexibility of the organic polymers in comparison with inorganic materials [17]. Moreover such membranes exhibit a limited durability in the presence of ozone [18]–[22]. The use of ceramic nanofilters permits to avoid these difficulties thanks to their good thermal, mechanical and chemical stability [23]. The successful deposition of very thin nanoporous layers of the targeted catalytic materials on nanoporous ceramic membranes has already been demonstrated [24].

The objective of the present work was to prepare a catalytic ceramic nanofilter with very low molecular weight cut-off (MWCO) and to demonstrate its operational performances. To do that, iron oxides have been chosen for several reasons: (i) they are identified in literature as ones of the most active catalysts [25]–[30], (ii) robust and low-cost sol-gel routes exist leading to stable colloidal suspensions [31], (iii) their toxicity is rather limited, (iv) they have been successfully used for the functionalization of ultrafiltration ceramic membranes [32]–[34]. A commercial nanofilter with a very

low MWCO of 200 Da was here functionalized by sol-gel deposition of a mesoporous maghemite γ-Fe_2O_3 thin layer. Preliminary experiments enabled to determine the maximum temperature usable for the thermal strengthening of the catalytic layer without significant permeance change. The catalytic activity of the maghemite equivalent powder was tested in batch reactor with ozone and para-chlorobenzoic acid (pCBA; MW = 156.6 Daltons), which quickly reacts with hydroxyl radicals formed with ozone at the catalyst surface, and only very slowly with ozone itself [33], [35]–[37]. The operational performance of the functionalized ceramic membrane was finally evaluated with a dedicated pilot. The obtained results unequivocally showed the catalytic activity of this functionalized membrane.

2. Experimental

2.1. Materials

Single channel tubular membranes used in this study were supplied by IKTS (Germany). They are 250 mm in length with internal and external diameters of 7 and 10 mm, respectively, and glass sealing of 13 mm on both ends. The effective filtration area (usable length x internal diameter x π) was equal to 4.9 10^{-3} m^2, with the separative layer on the inner side of the tube. Four intermediate layers are deposited between the titania-based microporous top layer and the α-Al_2O_3 macroporous support.

The maghemite (γ-Fe_2O_3) colloidal sol was synthetized according to the Massart's synthesis [31]. Synthesis details are given in supplementary information (SI).

The catalytic deposit was done by filling the membrane tube with the maghemite sol with a contact time of 4 min and a withdrawal rate of 10 cm min^{-1}. After drying at room temperature, the functionalized membranes were heated to 300 °C (maximum acceptable temperature considering the thermal stability of the selected ceramic nanofilter; see later) for one hour with a heating rate of 1 °C min^{-1}.

In order to obtained equivalent powder, the hydrosol was poured in a large beaker, dried at 60 °C and then heated to 300 °C for one hour with a heating rate of 1 °C min^{-1}.

2.2. Physicochemical characterization

The equivalent powder was analyzed by X-ray diffraction (XRD) and N_2 gas adsorption. Cross-section observations of pristine and functionalized membranes were done by scanning electron microscopy (SEM).

The N_2 molar permeance, P_e , across the membranes was determined at room temperature by measuring the molar flux density, J, as a function of transmembrane pressure, ΔP, in a dead-end module:

$$J = P_e \Delta P \qquad (1)$$

With: J, the molar flux density (mol m^{-2} s^{-1}); P_e, the molar permeance (mol m^{-2} s^{-1} Pa^{-1}); ΔP, the transmembrane pressure (Pa).

More details about these different experiments are given in supplementary information (SI).

2.3. Batch experiment with equivalent powder

In order to test the catalytic activity, pCBA aqueous solutions ([pCBA] = 2 or 3 µmol L^{-1} depending on the amount of catalyst used) were prepared. The pCBA concentration in water was analyzed by high-performance liquid chromatography (see SI for more details).

The ozone concentration in solution was determined by an amperometric O_3 micro-sensor (AMT Analysenmesstechnik GmbH) and by using the Indigo method [38] (see SI for more details).

For testing the catalytic activity of the equivalent powder, experiments were done in batch conditions. First, adsorption of pCBA on powder was investigated by mixing a pCBA solution ([pCBA]= 3 µmol L^{-1}) and powder ([γ-Fe_2O_3] = 3 g L^{-1}). After a contact time of one hour, the suspensions were filtered using PTFE syringe filters with a pore size of 0.2 µm and the filtrate solution was analyzed. Ozone produced by an ozone generator (Ozonia LAB2B, Suez, France) was continuously bubbled in a

Dreschel bottle containing a pCBA solution ([pCBA]= 3 µmol L^{-1}) and γ-Fe_2O_3 powder ([Fe_2O_3] = 3 g L^{-1}) under stirring. The ozone flux was equal to 20 L h^{-1} and the resulting gas concentration was $[O_3]_g$ = 11 g.Nm^{-3}. The concentration of dissolved ozone was about 4 mg O_3.L^{-1}. After one hour bubbling, the suspensions were filtered using PTFE syringe filters with a pore size of 0.2 µm and the filtrate solutions were analyzed.

2.4. Assessment of operational performance with a dedicated pilot

The schematic diagram of the home-made pilot and the protocol are given in SI. Experiments were carried out with or without pCBA ([pCBA] = 2 µmol.L^{-1}) in the feed tank. The concentration of the injected gaseous ozone was ~ 28 g.Nm^{-3}. The dissolved concentration of ozone in the transfer reactor and in all the experimental setup was ~3.5 mg O_3.L^{-1}. A phosphate buffer (NaH_2PO_4/Na_2HPO_4) was used to maintain the pH of the feed solution equal to 6.

Permeation measurements (pure water or pCBA solution) were done both on pristine and functionalized membranes, with a transmembrane pressure equal to 10 bars, and continuous weighting of the collected permeate during one hour. After each experiment, the membrane was rinsed with pure water and cleaned by filtration of ozonized water during 20 min. The pCBA retention, R_f(pCBA) was determined with the two types of membranes, with or without dissolved O_3, by measuring the pCBA concentration in the permeate and in the loop:

$$\boldsymbol{R_f(pCBA)} = \mathbf{1} - \left[\frac{\boldsymbol{C_{(pCBA,permeate)}}}{\boldsymbol{C_{(pCBA,loop)}}}\right] \qquad (2)$$

with: R_f(pCBA), the retention factor of pCBA by the membrane; $C_{(pCBA,\ loop)}$, the concentration of pCBA in the filtration loop; $C_{(pCBA,\ permeate)}$, the concentration of pCBA in the permeate.

As proposed by Elovitz and von Gunten [39], the R_{ct} concept was here employed:

$$\boldsymbol{R_{ct}} = \frac{\int_0^t [OH^\bullet]dt}{\int_0^t [O_3]dt} \qquad (3)$$

It is defined as the ratio of $OH^\bullet$ exposure to ozone exposure and quantifies the production of $OH^\bullet$ radicals More details are given in SI.

3. Results and discussion

3.1. Thermal stability of the selected ceramic nanofilter

To the best of our knowledge, the ceramic nanofiltration membrane selected for this study is the unique one commercially available with a very low MWCO of 200 Daltons. Such a low MWCO is required for the retention of the most current organic micropollutants exhibiting molecular weights of few hundred Daltons. Preliminary analyses showed that the titania-based microporous (pore size less than 2 nm) separative layer is amorphous. It can be thus suspected that its thermal stability in terms of microstructure and crystallinity is rather limited. Because the mechanical strengthening of the additional mesoporous catalytic layer requires a thermal treatment after deposition, it was decided to first investigate the thermal stability of the pristine membrane. A same membrane was successively treated for 30 min at different temperatures (from 200 °C to 800 °C). N_2 permeation measurements were then performed. Fig. 1 shows the variation of the N_2 permeance (determined from Equation (1)) as a function of the temperature of thermal treatment.

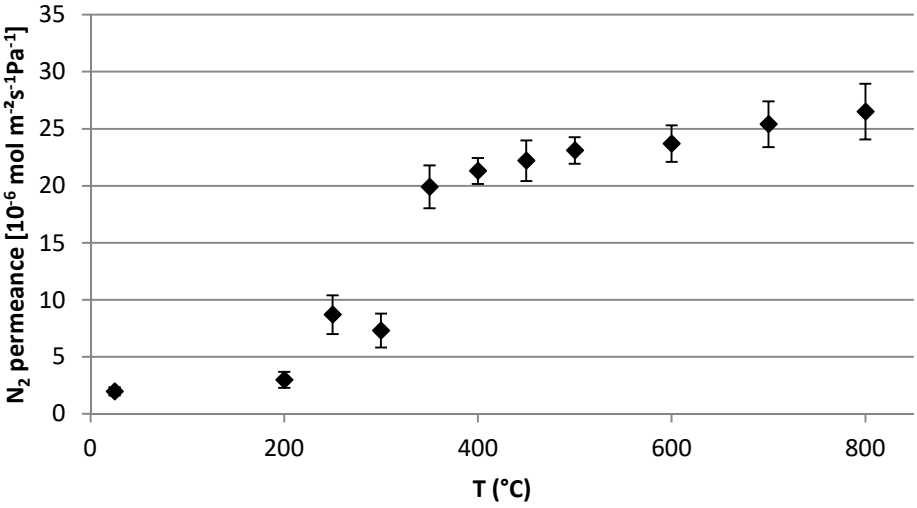

Fig. 1. N_2 permeance versus temperature of thermal treatment.

The N_2 permeance significantly increases between 300 and 350 °C. Assuming a viscous flow for nitrogen through the separative layer, a pressure drop across the overall membrane mainly due to its microporous separative layer, and considering the Darcy law (Equation (4)), it can be deduced that the increase of the membrane permeance is directly related to an increase of the intrinsic permeablity D of the microporous separative layer.

$$\boldsymbol{J = D\,\Delta P/\eta_f L} \qquad (4)$$

with: J, the flux density; D, the permeability of the microporous separative layer; ΔP, the transmembrane pressure; η_f, the dynamic viscosity of the fluid; L, the thickness of the separative layer.

From Carman-Kozeny relation, it appears that the permeability of a porous medium increases when its porosity or its pore size increases [40]. Considering the expected microstructural rearrangement for such a microporous layer with temperature [41], it can be deduced that the permeability increase is mainly due to an increase in the pore size and by way of consequence of the MWCO of the membrane. In order to prevent a change of the nanofilter performance, it was decided to limit to 300 °C the temperature of thermal strengthening of the deposited catalytic layer.

3.2. Characterization of the equivalent iron oxide powder

The physicochemical properties determined for the equivalent powder thermally treated at 300 °C are summarized in Table 1.

Table 1 Physicochemical properties of the equivalent powder thermally treated at 300 °C.

Colour	brick-red
Crystalline phase	γ-Fe_2O_3
Crystallite size (nm)	10.4 ± 0.1
BET specific area ($m^2\ g^{-1}$)	99 ± 1

As expected from the literature, its XRD pattern matches with that of maghemite, γ-Fe_2O_3 (Fig. 2). From the Full-Width Half-Maximum of the diffraction peaks and the Scherrer equation, the crystallite

size can be estimated as equal to 10.4 ± 0.1 nm. Assuming a set of identical spherical crystallites with such a diameter and considering that the maghemite bulk density is equal to 4.9 g cm^{-3}, the developed specific surface area is equal to 118 m^2 g^{-1}. This calculated value which neglects the area loss due to the contacts between nanoparticles is in rather good agreement with specific surface area experimentally measuring by the BET method, 99 ± 1 m^2 g^{-1}. Considering a random close packing arrangement of the nanocrystallites, the expected porosity is around 40 % and the average pore size equal to around one third of the size of the crystallites, i.e. ~ 3.5 nm (mesopores).

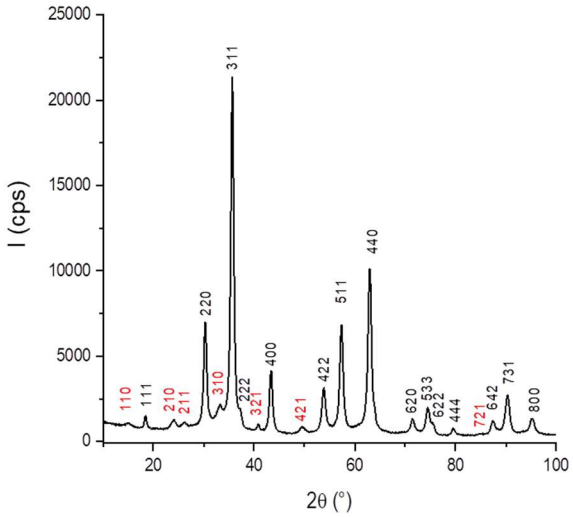

Fig. 2. XRD pattern of the equivalent powder thermally treated at 300 °C.
(peaks with Miller indexes hkl written in black: common peaks between maghemite γ-Fe_2O_3 and magnetite Fe_3O_4; peaks with Miller indexes hkl written in red: specific peaks of maghemite).

The maghemite powder was then tested in presence of an adapted concentration of pCBA and ozone in order to quantify its catalytic activity. pCBA retention by adsorption and elimination by ozonation with and without catalyst are presented in Fig. 3. As previously mentioned, the pCBA elimination is directly related to the production of $OH^{\bullet}$ thanks to the presence of the catalyst. As expected without catalyst, the pCBA degradation is very low because very few $OH^{\bullet}$ were formed. Fig. 3 highlights i) a very low adsorption of pCBA on the powder, ii) an important generation of hydroxyl radicals when ozone was injected in presence of the selected catalyst iii) pCBA displays slow reaction rates with ozone. These results confirm that this material is a good candidate for the functionalization of the ceramic nanofilter.

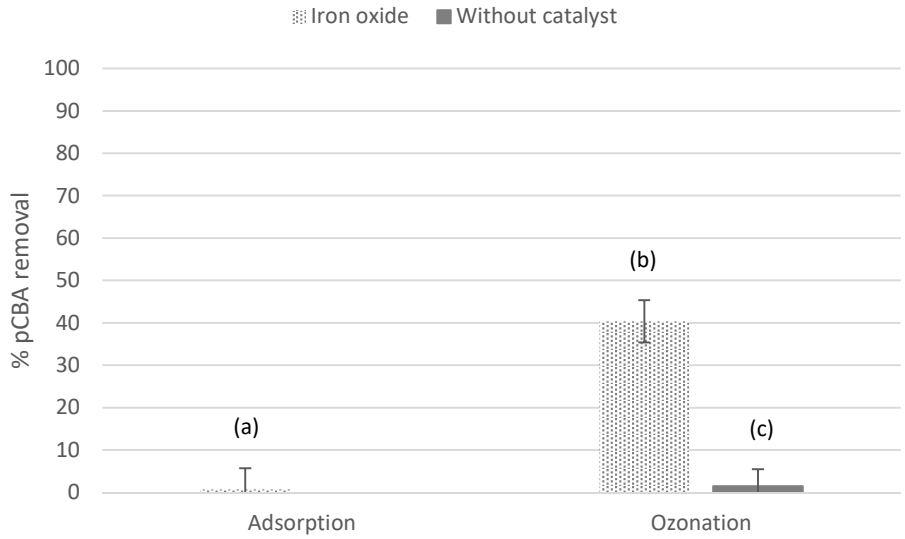

Fig. 3. pCBA removal by the equivalent powder and without after one hour of contact time.
(a) pCBA retention by adsorption ($[Fe_2O_3]$=3 g L^{-1}, $[pCBA]_0$= 3 µmol L^{-1});
(b) pCBA elimination by $OH^{\bullet}$ resulting from catalytic ozonation ($[Fe_2O_3]$=3 g L^{-1}, $[pCBA]_0$= 3 µmol L^{-1}, Q_{gasO3}=20 L h^{-1}, $[O_3]$=11 g Nm^{-3}).
(c) pCBA elimination by ozonation ($[Fe_2O_3]$=0 g L^{-1}, $[pCBA]_0$= 5 µmol L^{-1}, Q_{gasO3}=20 L h^{-1}, $[O_3]$=10 g Nm^{-3})

3.3. Microstructural observation of the modified membranes

Fig. 4 shows a SEM image of the functionalized membrane cross-section. It is focused close to the inner side of the single channel tube. It is possible to identify one part of the third intermediate layer, the fourth intermediate layer, the microporous titania-based top layer (thickness of ~ 110 nm) and the additional mesoporous maghemite layer exhibiting a uniform thickness of ~ 80 nm.

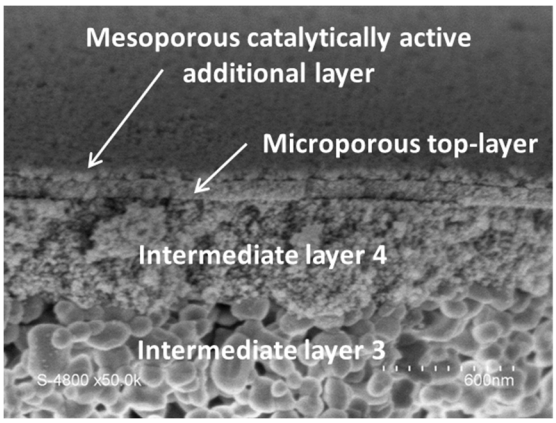

Fig. 4. SEM cross-section image of the functionalized ceramic nanofilter close to the inner side.

3.4. Operational performance of the modified membranes

The permeance values for pure water and a pCBA aqueous solution were measured using the hybrid pilot, with a pristine membrane or a functionalized membrane, and with or without ozone injection (Fig. 5). The permeance values were quite stable during all the experiments (one hour long). Using pure water without ozone, the permeance was not significantly modified by the membrane functionalization (~ 10 L (h m^2 bar)$^{-1}$. Injection of ozone induces a measurable decrease of permeance only for the pristine membrane. This unexpected result is difficult to explain. It could possibly be assigned to a weak change of pH due to ozone injection, knowing that complex electrokinetic phenomena occur during the forced flow of ionic solutions inside nanopores [42]. This effect would

not be observed with the functionalized membrane due to a decomposition of ozone in hydroxyl radicals during the crossing the catalytic layer. Another, but less substantiated, explanation would be the possible presence of ozone nanobubbles inside the micropores of the titania layer inducing a partial pore blocking effect and consequently the observed permeance reduction. In fact, nucleation of such ozone nanobubbles would be explained by the confinement of the ozone-saturated water in these very small pores [43]. The permeance values for the pristine and functionalized membranes with the pCBA solution are quite the same, around 9 L (h m² bar)$^{-1}$. This decrease compared to pure water is usually observed. With ozone injection, as for pure water, the permeance is higher for the functionalized membrane than for the pristine one (~ 8.0 versus ~ 6.5 L (h m² bar)$^{-1}$).

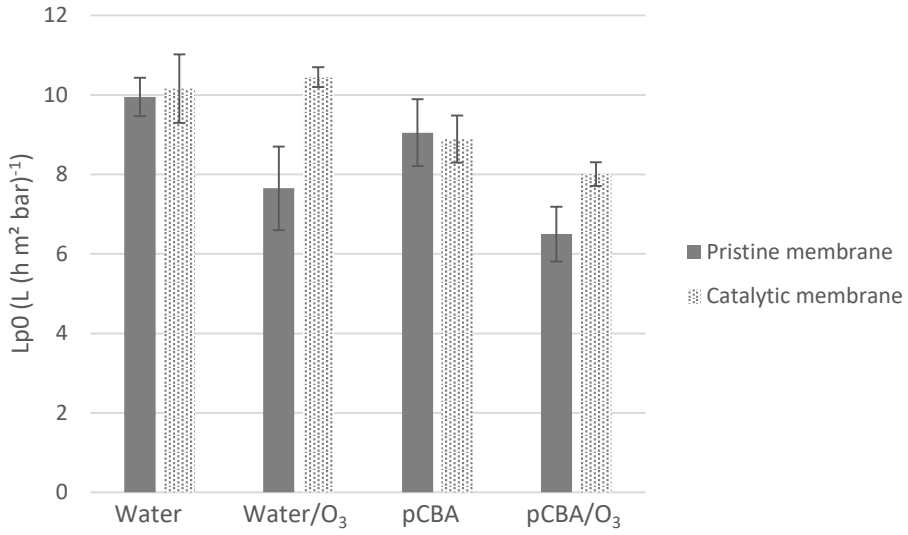

Fig. 5. Permeance values after 1h for pure water and a pCBA aqueous solution ($[pCBA]_0$= 2 µmol L^{-1}) with a pristine membrane and a functionalized membrane, with or without ozone injection.

In absence of ozone, the retention factor R_f (pCBA) is larger for the functionalized membrane (~ 65 %) than for the pristine one (~ 50 %). Considering that the pH of the treated solution was maintained close to 6 and that the pKa of pCBA is equal to 4, it means than this compound was mainly present in its deprotonated negative form. On the other hand, the zero point of charge (ZPC) of titania depends on its crystalline nature. It is located between 4 and 5 for rutile form and between 6 and 7 for anatase form [44], [45]. For maghemite (γ-Fe_2O_3), the ZPC is in the range from 6 to 9 [45]. Based on all these data, it can be concluded that a pH equal to 6 is more favourable to the development of positively charged surfaces in the case of γ-Fe_2O_3 and by way of consequence to an electrostatic attraction of the negatively-charged molecules of pCBA.

The pCBA degradation by ozone using pristine or functionalized membranes is illustrated in Fig. 6 and the calculation details are given in SI. It is clearly enhanced with the catalytic membrane which favours the production of $OH^{\bullet}$.

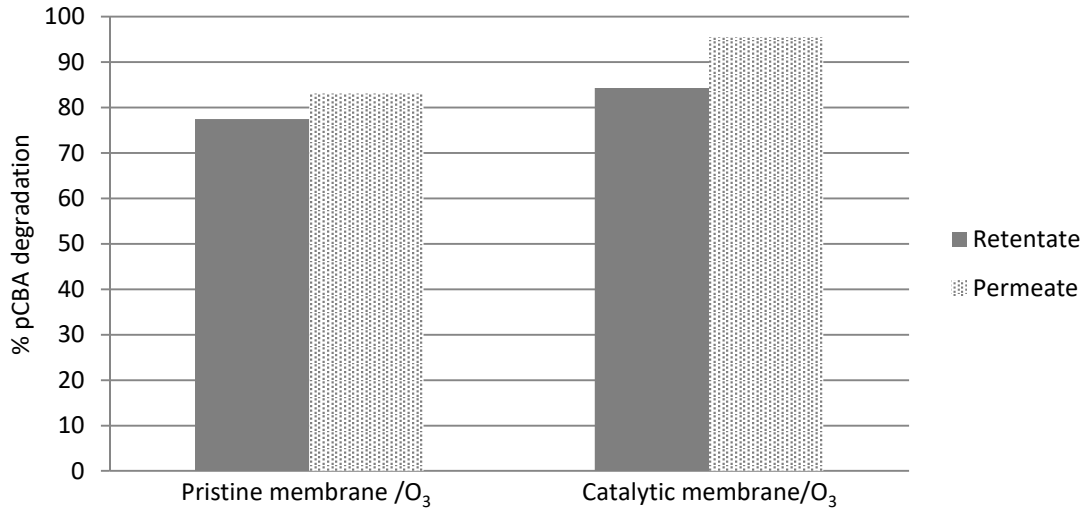

Fig. 6. Percentage of the pCBA elimination for the pristine and catalytic membrane in presence of ozone in permeate and retentate after 2.5h.

In order to quantify the catalytic performance of the functionalized membrane, the R_{ct} value was determined by plotting the pCBA elimination as a function of O_3 exposure (Fig. 7). As reference a configuration without membrane was also implemented. In such a case, R_{ct} is quite low ($2.58\ 10^{-10}$). With the pristine membrane, R_{ct} increases to $4.26\ 10^{-10}$. The pristine membrane thus exhibits a weak catalytic activity. The larger value of R_{ct}, $1.49\ 10^{-9}$, is obtained for the functionalized membrane. These results undoubtedly demonstrate the significant enhancement of the catalytic ozonation due the presence of the added mesoporous maghemite thin layer.

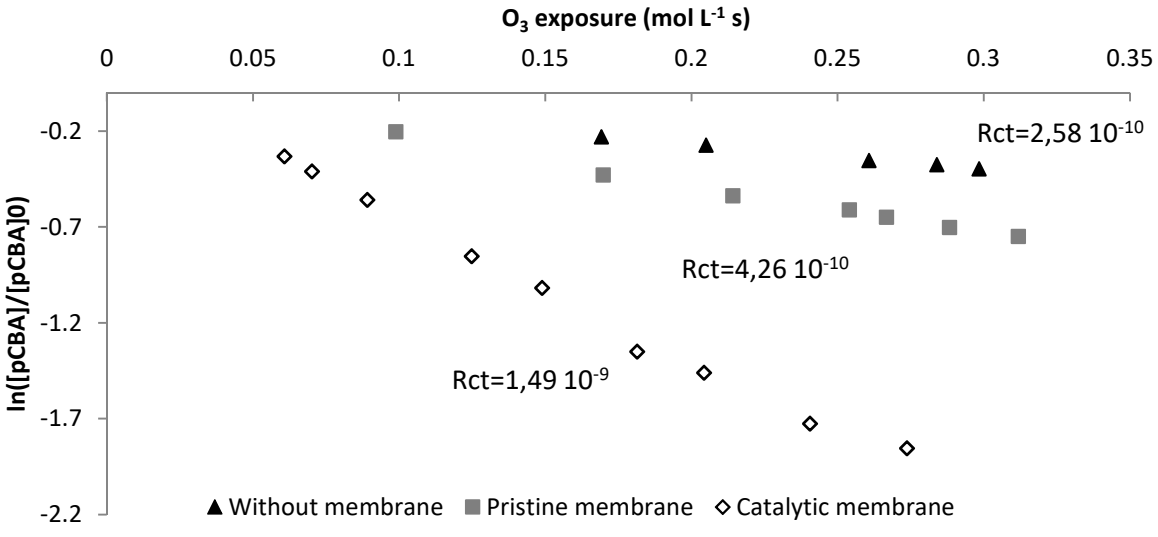

Fig. 7. Quantification of the elimination of the pCBA versus O_3 exposure in the pilot loop for different configurations in order to determine R_{ct} values.

4. Conclusions

Direct coupling between nanofiltration and catalytic ozonation is a very promising approach for solving the emerging issue of micropollutant elimination in water. The associated key parameters are the development of performing nanofilters exhibiting a low MWCO, an excellent durability in presence of ozone and a high catalytic activity. In this context, a commercial ceramic nanofilter with

a MWCO equal to 200 Daltons has been selected and was successfully functionalized using a simple a robust method consisting in the deposition of mesoporous maghemite thin layer on the microporous top-layer of the nanofilter. The preliminary results show that it is possible to functionalize this ceramic nanofilter without disturbing its filtration features. They also demonstrate the good catalytic activity of the deposited iron oxide. Despite a non-optimized design of the used pilot, a significant enhancement of the catalytic activity has been evidenced for the functionalized nanofilter.

The future experiments will deal with the implementation of this functionalized nanofilter for the treatment of aqueous solutions containing one or several micropollutants. Both micropollutant elimination, and also membrane fouling, will be considered for the assessment of its operational performance.

Acknowledgements

The authors warmly thank the French National Agency for Research (ANR) for the financial support of this study through the ANR JCJC 2016 project Saware (ANR-16-CE-04-0002-01).

References

[1] (UNDP) United Nations Development Programme, "Human Development Report 2006, beyond scarcity: power, poverty and the global water crisis." 2006, [Online]. Available: http://www.undp.org/content/dam/undp/library/corporate/HDR/2006%20Global%20HDR/HDR-2006-Beyond%20scarcity-Power-poverty-and-the-global-water-crisis.pdf.

[2] European Environement Agency, "European Water policies and human health - Combining reported environmental information." No 32/2016, 2016, [Online]. Available: https://www.eea.europa.eu/publications/public-health-and-environmental-protection.

[3] M. J. Benotti, R. A. Trenholm, B. J. Vanderford, J. C. Holady, B. D. Stanford, and S. A. Snyder, "Pharmaceuticals and Endocrine Disrupting Compounds in U.S. Drinking Water," *Environ. Sci. Technol.*, vol. 43, no. 3, pp. 597–603, Feb. 2009, doi: 10.1021/es801845a.

[4] N. Ratola, A. Cincinelli, A. Alves, and A. Katsoyiannis, "Occurrence of organic microcontaminants in the wastewater treatment process. A mini review," *Journal of Hazardous Materials*, vol. 239–240, pp. 1–18, Nov. 2012, doi: 10.1016/j.jhazmat.2012.05.040.

[5] A. Matilainen, M. Vepsäläinen, and M. Sillanpää, "Natural organic matter removal by coagulation during drinking water treatment: A review," *Advances in Colloid and Interface Science*, vol. 159, no. 2, pp. 189–197, Sep. 2010, doi: 10.1016/j.cis.2010.06.007.

[6] G. Crini, "Non-conventional low-cost adsorbents for dye removal: A review," *Bioresource Technology*, vol. 97, no. 9, pp. 1061–1085, Jun. 2006, doi: 10.1016/j.biortech.2005.05.001.

[7] M. Sillanpää, M. C. Ncibi, A. Matilainen, and M. Vepsäläinen, "Removal of natural organic matter in drinking water treatment by coagulation: A comprehensive review," *Chemosphere*, vol. 190, pp. 54–71, Jan. 2018, doi: 10.1016/j.chemosphere.2017.09.113.

[8] A. K. Verma, R. R. Dash, and P. Bhunia, "A review on chemical coagulation/flocculation technologies for removal of colour from textile wastewaters," *Journal of Environmental Management*, vol. 93, no. 1, pp. 154–168, Jan. 2012, doi: 10.1016/j.jenvman.2011.09.012.

[9] F. Renault, B. Sancey, P.-M. Badot, and G. Crini, "Chitosan for coagulation/flocculation processes – An eco-friendly approach," *European Polymer Journal*, vol. 45, no. 5, pp. 1337–1348, May 2009, doi: 10.1016/j.eurpolymj.2008.12.027.

[10] R. Singh, "Chapter 2 - Water and Membrane Treatment," in *Membrane Technology and Engineering for Water Purification (Second Edition)*, R. Singh, Ed. Oxford: Butterworth-Heinemann, 2015, pp. 81–178.

[11] H. A. van der Sloot, D. S. Kosson, and O. Hjelmar, "Characteristics, treatment and utilization of residues from municipal waste incineration," *Waste Management*, vol. 21, no. 8, pp. 753–765, Jan. 2001, doi: 10.1016/S0956-053X(01)00009-5.

[12] C. Mansas, J. Mendret, S. Brosillon, and A. Ayral, "Coupling catalytic ozonation and membrane separation: A review," *Separation and Purification Technology*, vol. 236, p. 116221, Apr. 2020, doi: 10.1016/j.seppur.2019.116221.

[13] R. Gracia, J. L. Aragües, and J. L. Ovelleiro, "Study of the Catalytic Ozonation of Humic Substances in Water and Their Ozonation Byproducts," *Ozone: Science & Engineering*, vol. 18, no. 3, pp. 195–208, Jan. 1996, doi: 10.1080/01919519608547326.

[14] S. Cortés, J. Sarasa, P. Ormad, R. Gracia, and J. L. Ovelleiro, "Comparative Efficiency of the Systems O3/High pH And 03/catalyst for the Oxidation of Chlorobenzenes in Water," *Ozone: Science & Engineering*, vol. 22, no. 4, pp. 415–426, Aug. 2000, doi: 10.1080/01919510009408784.

[15] J. H. Owens *et al.*, "Pilot-Scale Ozone Inactivation of Cryptosporidium and Other Microorganisms in Natural Water," *Ozone: Science & Engineering*, vol. 22, no. 5, pp. 501–517, 2000, doi: 10.1080/01919510009408793.

[16] U. von Gunten, "Ozonation of drinking water: Part I. Oxidation kinetics and product formation," *Water Research*, vol. 37, no. 7, pp. 1443–1467, Apr. 2003, doi: 10.1016/S0043-1354(02)00457-8.

[17] J. Hora, C. Hall, D. Evans, and E. Charrault, “Inorganic Thin Film Deposition and Application on Organic Polymer Substrates,” *Advanced Engineering Materials*, vol. 20, no. 5, p. 1700868, May 2018, doi: 10.1002/adem.201700868.
[18] Y. Mori, T. Oota, M. Hashino, M. Takamura, and Y. Fujii, “Ozone-microfiltration system,” *Desalination*, vol. 117, no. 1, pp. 211–218, Sep. 1998, doi: 10.1016/S0011-9164(98)00098-8.
[19] S. Bamperng, T. Suwannachart, S. Atchariyawut, and R. Jiraratananon, “Ozonation of dye wastewater by membrane contactor using PVDF and PTFE membranes,” *Separation and Purification Technology*, vol. 72, no. 2, pp. 186–193, Apr. 2010, doi: 10.1016/j.seppur.2010.02.006.
[20] P. Luis, M. Saquib, C. Vinckier, and B. Van der Bruggen, “Effect of Membrane Filtration on Ozonation Efficiency for Removal of Atrazine from Surface Water,” *Ind. Eng. Chem. Res.*, vol. 50, no. 14, pp. 8686–8692, Jul. 2011, doi: 10.1021/ie200375j.
[21] H. Vatankhah, C. C. Murray, J. W. Brannum, J. Vanneste, and C. Bellona, “Effect of pre-ozonation on nanofiltration membrane fouling during water reuse applications,” *Separation and Purification Technology*, vol. 205, pp. 203–211, Oct. 2018, doi: 10.1016/j.seppur.2018.03.052.
[22] L. Flyborg, B. Björlenius, and K. M. Persson, “Can treated municipal wastewater be reused after ozonation and nanofiltration? Results from a pilot study of pharmaceutical removal in Henriksdal WWTP, Sweden,” *Water Science and Technology*, vol. 61, no. 5, pp. 1113–1120, Mar. 2010, doi: 10.2166/wst.2010.029.
[23] A. Ayral, A. Julbe, and C. Guizard, *Chap.25 - Ceramic membrane processing; new approaches in their design and applications*, B.I. Lee and S. Komarneni. Boca Raton, USA: Taylor ans Francis Group, 2005.
[24] J. Gwak *et al.*, “Porous ceramic membranes exhibiting ferri/ferromagnetic properties for separation,” *Separation and Purification Technology*, vol. 46, no. 1, pp. 118–124, Nov. 2005, doi: 10.1016/j.seppur.2005.05.002.
[25] A. Lv, C. Hu, Y. Nie, and J. Qu, “Catalytic ozonation of toxic pollutants over magnetic cobalt-doped Fe3O4 suspensions,” *Applied Catalysis B: Environmental*, vol. 117–118, pp. 246–252, 2012, doi: https://doi.org/10.1016/j.apcatb.2012.01.020.
[26] S. Zhu, B. Dong, Y. Yu, L. Bu, J. Deng, and S. Zhou, “Heterogeneous catalysis of ozone using ordered mesoporous Fe3O4 for degradation of atrazine,” *Chemical Engineering Journal*, vol. 328, pp. 527–535, 2017, doi: https://doi.org/10.1016/j.cej.2017.07.083.
[27] Y. D. Shahamat, M. Farzadkia, S. Nasseri, A. H. Mahvi, M. Gholami, and A. Esrafili, “Magnetic heterogeneous catalytic ozonation: a new removal method for phenol in industrial wastewater,” *Journal of Environmental Health Science and Engineering*, vol. 12, no. 1, p. 50, Feb. 2014, doi: 10.1186/2052-336X-12-50.
[28] S.-P. Tong, R. Shi, H. Zhang, and C. Ma, “Kinetics of Fe3O4–CoO/Al2O3 catalytic ozonation of the herbicide 2-(2,4-dichlorophenoxy) propionic acid,” *Journal of Hazardous Materials*, vol. 185, no. 1, pp. 162–167, 2011, doi: https://doi.org/10.1016/j.jhazmat.2010.09.013.
[29] C. Cooper and R. Burch, “An investigation of catalytic ozonation for the oxidation of halocarbons in drinking water preparation11The research was performed in the Catalysis Research Group, Department of Chemistry, University of Reading, Berkshire RG6 6AD, U.K.,” *Water Research*, vol. 33, no. 18, pp. 3695–3700, 1999, doi: https://doi.org/10.1016/S0043-1354(99)00091-3.
[30] R. Yuan, B. Zhou, D. Hua, and C. Shi, “Enhanced photocatalytic degradation of humic acids using Al and Fe co-doped TiO2 nanotubes under UV/ozonation for drinking water purification,” *Journal of Hazardous Materials*, vol. 262, pp. 527–538, 2013, doi: https://doi.org/10.1016/j.jhazmat.2013.09.012.
[31] A. Bee, R. Massart, and S. Neveu, “Synthesis of very fine maghemite particles,” *Journal of Magnetism and Magnetic Materials*, vol. 149, no. 1, pp. 6–9, Aug. 1995, doi: 10.1016/0304-8853(95)00317-7.

[32] B. S. Karnik, S. H. Davies, M. J. Baumann, and S. J. Masten, "Fabrication of Catalytic Membranes for the Treatment of Drinking Water Using Combined Ozonation and Ultrafiltration," *Environ. Sci. Technol.*, vol. 39, no. 19, pp. 7656–7661, Oct. 2005, doi: 10.1021/es0503938.

[33] H. Park, Y. Kim, B. An, and H. Choi, "Characterization of natural organic matter treated by iron oxide nanoparticle incorporated ceramic membrane-ozonation process," *Water Research*, vol. 46, no. 18, pp. 5861–5870, Nov. 2012, doi: 10.1016/j.watres.2012.07.039.

[34] S. Byun *et al.*, "Mn oxide coated catalytic membranes for a hybrid ozonation–membrane filtration: Comparison of Ti, Fe and Mn oxide coated membranes for water quality," *Water Research*, vol. 45, no. 1, pp. 163–170, 2011, doi: https://doi.org/10.1016/j.watres.2010.08.031.

[35] K. Ibn Abdul Hamid, P. J. Scales, S. Allard, J.-P. Croue, S. Muthukumaran, and M. Duke, "Ozone combined with ceramic membranes for water treatment: Impact on HO radical formation and mitigation of bromate," *Journal of Environmental Management*, vol. 253, p. 109655, Jan. 2020, doi: 10.1016/j.jenvman.2019.109655.

[36] H. Park, J. Kim, H. Jung, J. Seo, and H. Choi, "Iron Oxide Nanoparticle-Impregnated Alumina for Catalytic Ozonation of para-Chlorobenzoic Acid in Aqueous Solution," *Water, Air, & Soil Pollution*, vol. 225, no. 6, p. 1975, May 2014, doi: 10.1007/s11270-014-1975-0.

[37] J.-S. Park, H. Choi, and J. Cho, "Kinetic decomposition of ozone and para-chlorobenzoic acid (pCBA) during catalytic ozonation," *Water Research*, vol. 38, no. 9, pp. 2285–2292, May 2004, doi: 10.1016/j.watres.2004.01.040.

[38] H. Bader and J. Hoigné, "Determination of ozone in water by the indigo method," *Water Research*, vol. 15, no. 4, pp. 449–456, Jan. 1981, doi: 10.1016/0043-1354(81)90054-3.

[39] M. S. Elovitz and U. von Gunten, "Hydroxyl Radical/Ozone Ratios During Ozonation Processes. I. The Rct Concept," *Ozone: Science & Engineering*, vol. 21, no. 3, pp. 239–260, Jan. 1999, doi: 10.1080/01919519908547239.

[40] C. J. Brinker and G. W. Scherer, *Sol-Gel Science The Physics and Chemistry of Sol-Gel Processing*. Elsevier Inc., 1990.

[41] J. Sekulic, J. E. ten Elshof, and D. H. A. Blank, "Synthesis and Characterization of Microporous Titania Membranes," *Journal of Sol-Gel Science and Technology*, vol. 31, no. 1, pp. 201–204, Aug. 2004, doi: 10.1023/B:JSST.0000047987.50901.15.

[42] C. Mazzoni, F. Orlandini, and S. Bandini, "Role of electrolyte type on TiO2–ZrO2 nanofiltration membranes performances," *Desalination*, vol. 240, no. 1, pp. 227–235, May 2009, doi: 10.1016/j.desal.2007.11.074.

[43] S. Bories and M. Prat, "11 - Isothermal Nucleation and Bubble Growth in Porous Media at Low Supersaturations," in *Transport Phenomena in Porous Media II*, D. B. Ingham and I. Pop, Eds. Oxford: Pergamon, 2002, pp. 276–315.

[44] G. A. Parks and P. L. de Bruyn, "THE ZERO POINT OF CHARGE OF OXIDES1," *J. Phys. Chem.*, vol. 66, no. 6, pp. 967–973, Jun. 1962, doi: 10.1021/j100812a002.

[45] M. Kosmulski, "Isoelectric points and points of zero charge of metal (hydr)oxides: 50years after Parks' review," *Advances in Colloid and Interface Science*, vol. 238, pp. 1–61, Dec. 2016, doi: 10.1016/j.cis.2016.10.005.